ESRF	**Experiment title:** Magnetic excitations across the Mott Insulator - Metal Transition in $(Sr_{1-x}La_x)_3Ir_2O_7$	**Experiment number**: HC2244
Beamline:	**Date of experiment**: from: 17.02.2016 to: 23.02.2016	**Date of report**: 02.09.2016
Shifts:	**Local contact(s)**: Marco Moretti Sala	*Received at ESRF:*

Names and affiliations of applicants (* indicates experimentalists):

Xingye Lu, D. E. McNally, T. Schmitt

Department of Synchrotron Radiation and Nanotechnology, Paul Scherrer Institut, CH-5232 Villigen PSI, Switzerland

Report:

We use resonant elastic and inelastic X-ray scattering at Ir-*L*3 edge on ID20 of ESRF to study the doping-dependent magnetic order, magnetic excitations and spin-orbit excitons in the bilayer iridate $(Sr_{1-x}La_x)_3Ir_2O_7$ ($0 \leq x \leq 0.065$). With increasing doping *x*, the three-dimensional (3D) long range antiferromagnetic order (LAF) is gradually suppressed and evolves into a short range order (SAF) from $x = 0$ to 0.05, followed by a transition from 3D SAF to 2D SAF between $x = 0.05$ and 0.065. Following the evolution of the antiferromagnetic order, the magnetic excitations undergo damping, anisotropic softening and gap collapse. From the lack of *c*-axis magnetic correlations in $x = 0.065$, we conclude that electron doping suppresses the interlayer couplings and drives $(Sr_{1-x}La_x)_3Ir_2O_7$ into a 2D SAF correlated metallic state hosting strong antiferromagnetic spin fluctuations. Meanwhile, the spin-orbit excitons at (½, 0) decrease in energy by ~70 meV across the transition from 3D to 2D SAF, suggesting that magnetic correlations are crucial for stabilizing the Mott gap.

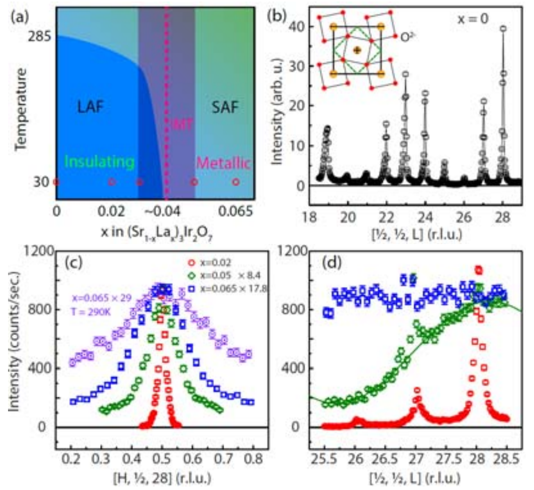

Figure 1 (a) Schematic phase diagram of $(Sr_{1-x}La_x)_3Ir_2O_7$. The dopings used in present study are marked by red circles. (b) *L* scan of the *c*-axis *G*-type antiferromagnetic order for $x = 0$. (c), (d) Doping dependent *H* and *L* scans across the magnetic Bragg peak (1/2, 1/2, 28). All the measurements were performed at 30 K unless otherwise indicated.

Figure 1 describes the doping evolution of the magnetic order. Figure 1(a) is a schematic magnetic and electronic phase diagram of $(Sr_{1-x}La_x)_3Ir_2O_7$. The doping levels *x* measured at $T = 30$ K are indicated by red circles. We have measured the magnetic Bragg peaks along [H, ½, 28] and [½, ½, L] for $x = 0$, 0.02, 0.05, and 0.065 using the elastic channel of the RIXS spectrometer. The *L* scan for $x = 0$ displays magnetic Bragg peaks from $L = 19$ to 28 with an intensity modulation, in agreement with previous reports [1]. Upon electron doping, the 3D LAF persists for $x = 0.02$ but becomes short ranged for $x = 0.05$, as indicated by the broad peaks along both *H* and *L* in Figs. 1(c) and 1(d). The *L* scan for the metallic $x = 0.05$ sample reveals a broad feature superimposed on a flat background, and is well fitted by a sum of the bilayer antiferromagnetic structural factor [1] and a constant background [green solid curve in Fig. 1(d)]. The presence of this broad feature indicates that the magnetic correlation length along *c* axis has decreased to a very small value comparable with the bilayer distance. This hints that the *c*-axis magnetic correlations supporting the *G*-type AFM are on the verge of disappearing, although the interlayer coupling is still present. The constant background can be attributed to a vanishing of the 3D SAF in a partial volume of the sample. This is in agreement with the percolative nature of the IMT, assuming that charge carriers are suppressing the magnetic order. For $x = 0.065$, the *L* scan becomes featureless while the broader in-plane magnetic Bragg peak remains and persists at 290K [Fig.1(c) and 1(d)]. This indicates that further doping destroys the interlayer couplings that support the 3D SAF and drives the system into a robust 2D SAF state. This corroborates our explanation of the L scan for $x = 0.05$.

Figure 2 shows the doping-dependent magnetic excitations and the spin-orbit excitons. The in-plane momentum dependent RIXS for $x = 0$, 0.02 and 0.065 are shown as color maps in Figs. 2(a)-(c). For $x = 0$, the overall dispersion, large magnon gap and spectral-weight distribution are consistent with a previous report measured at the same L [2]. In addition, our results reveal clear dispersive spin-orbit excitons. With increasing La concentration, the magnetic excitations are damped: they broaden in energy and decrease in intensity. The intensity and dispersion of the magnetic excitations exhibit a strong doping dependence [Figs. 2 and 3]. The dispersions are symmetric about (1/4, 1/4) and change less from $x = 0$ to $x = 0.03$. Across the IMT to $x = 0.05$, the dispersion becomes asymmetric with a different gap size at (1/2, 1/2) and (0, 0). A substantial softening occurs along (1/2, 1/2)-(1/4, 1/4) while the band top at (1/2, 0) remains unchanged. This anisotropic softening is followed by a further softening at (1/4, 1/4) and, surprisingly, a sizable hardening at (1/2, 0) in $x = 0.065$ [Figs. 2 and 3]. Furthermore, the large magnon gap in $x > 0.05$ collapses dramatically in $x = 0.065$, where the magnetic excitations at (1/2, 1/2) overlap with the elastic magnetic scattering, whereas a weak signal is observed at (0, 0).

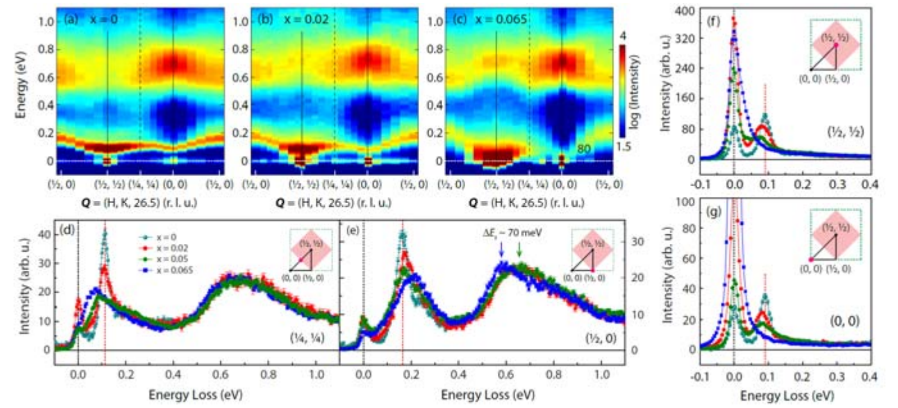

Figure 2 (a)-(c) In-plane momentum dependence of RIXS spectra of $x = 0$, $x = 0.02$ and 0.065. (d)-(e) Comparison of the magnetic excitations and spin-orbit excitons between $x = 0$, 0.02, 0.05 and 0.065 at (1/4, 1/4) and (1/2, 1/2). (f)-(g) Doping dependence of the magnetic excitations at (1/2, 1/2) and (0, 0). The blue and green arrows in (e) show the peak positions of the spin-orbit excitons and ΔE_s marks the energy difference of the peak positions.

We have extracted the magnon dispersions and fitted the dispersions according to the bilayer model [2], the J-J_2-J_3 model [3] and the quantum dimer model [4], as shown in Fig. 3. The detailed analysis and related discussions have been described in our manuscripte 'X. Lu *et al.*, arxiv:1608.06208'. A comparison between our results and La doped Sr_2IrO_4 [3] indicates that the doped itinerant electrons suppress the AFM by weakening the magnetic couplings and drive the system into a 2D SAF correlated metallic state hosting strong AFM spin fluctuations.

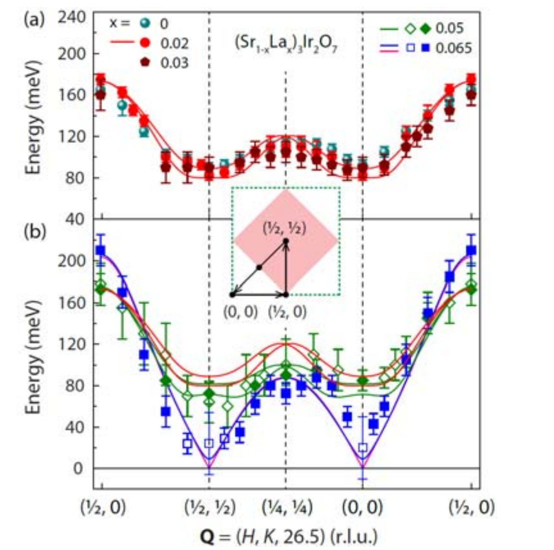

Figure 3 Doping dependent dispersions of magnetic excitations for $(Sr_{1-x}La_x)_3Ir_2O_7$ ($x = 0$, 0.02, 0.03, 0.05 and 0.065). The red, green and blue curves fits the dispersions for $x = 0.02$, 0.05 and 0.065 using bilayer model [2], respectively. The pink curve is a fitting of the dispersion for 0.065 according to the J-J_2-J_3 model [3].

References:
[1] J. W. Kim *et al.*, Phys. Rev. Lett. **109**, 037204 (2012).
[2] J. Kim *et al.*, Phys. Rev. Lett. **109**, 157402 (2012).
[3] H. Gretarsson *et al.*, arXiv:1603.07547 (2016).
[4] M. Moretti Sala *et al.*, Phys. Rev. B **92**, 024405 (2015).